NASA TECHNICAL NOTE

INVESTIGATION OF OPENING CHARACTERISTICS OF AN ALL-FLEXIBLE PARAWING

by Thomas G. Gainer

Langley Research Center
Langley Station, Hampton, Va.

NATIONAL AERONAUTICS AND SPACE ADMINISTRATION • WASHINGTON, D. C. • FEBRUARY 1969

INVESTIGATION OF OPENING CHARACTERISTICS

OF AN ALL-FLEXIBLE PARAWING

By Thomas G. Gainer

Langley Research Center
Langley Station, Hampton, Va.

NATIONAL AERONAUTICS AND SPACE ADMINISTRATION

INVESTIGATION OF OPENING CHARACTERISTICS

OF AN ALL-FLEXIBLE PARAWING

By Thomas G. Gainer
Langley Research Center

SUMMARY

Opening forces for an all-flexible parawing were measured during deployments made in the 17-foot (5.18 m) section of the Langley 300-MPH 7- by 10-foot tunnel. The wing tested had a nominal keel length of 5 feet (1.524 m), a flat-pattern leading-edge sweep of 45°, and equal-length leading edges and keel. Lift- and drag-coefficient time histories were obtained by measuring three components of the total force on the wing. Tunnel dynamic pressure was varied from 0.5 to 2.0 pounds per square foot (24.0 to 95.8 N/m^2). Two slotted versions of the wing were also tested and some exploratory tests of a reefing technique of shortening one of the keel suspension lines were made. The results indicated that as the wing opened, there was a buildup in both lift and drag coefficient to large values. The ratio of maximum resultant-force coefficient to steady-state resultant-force coefficient (shock factor) was about 3.0. When the resultant force reached a maximum, it was inclined about 48° to the airstream. For the infinite mass conditions of the tests, filling time was about 2.5 times the ratio of keel length to velocity. The complete force time history, including both the opening force and the forces during the transition to steady-state angle of attack, could be nondimensionalized with respect to filling time. Opening forces for a 5-foot (1.524 m) wing calculated by using the wind-tunnel data were in excellent agreement with drop-test data. The two slotted wings gave no significant reductions in opening force over those obtained for the unslotted wing. Pulling in on one of the keel suspension lines produced a significant reduction in opening force.

INTRODUCTION

Completely flexible parawings are receiving a great deal of attention for applications such as spacecraft recovery and air dropping of cargo and personnel. These all-flexible parawings are capable of providing gliding, controllable flight by proper rigging of multiple suspension lines which connect the wing to the payload. In contrast to previous parawing designs (refs. 1 and 2), the all-flexible parawing (refs. 3, 4, and 5) does not have rigid or inflatable structural members, and therefore it is much easier to construct,

package, and deploy. Lift-drag ratios for the all-flexible wings, on the other hand, are still relatively high. Completely flexible wings being tested at the Langley Research Center have developed lift-drag ratios above 3. Sink rates for this lift-drag ratio can be low enough to ensure a spacecraft land-recovery system that does not use retrorockets or a flare maneuver. Also, this relatively high lift-drag ratio can provide men and cargo dropped from aircraft with a substantial zero-wind glide range and maneuvering capability that they do not now have with conventional parachutes. Because of the interest being shown in these wings, a number of wind-tunnel and model flights are being made to investigate their stability, control, performance, opening reliability, and opening shock loads. The purpose of the present paper is to present the results of experimental wind-tunnel opening loads and to correlate these studies with available flight data.

The present investigation was made in the 17-foot (5.18 m) test section of the Langley 300-MPH 7- by 10-foot tunnel. All-flexible parawings with a nominal keel length of 5 feet (1.524 m) equal length leading edges and keel, and flat-pattern sweep of 45° were deployed in the tunnel. Time histories of three components of the total load in the suspension lines — two components normal to the direction of flow and a third component along the direction of flow — were recorded. Time histories of opening load, the ratio of maximum opening load to the steady-state flight load of each wing, and variation of canopy inflation time with tunnel velocity were obtained. This type of information is used for parachutes to estimate opening shock loads for almost any deployment conditions as indicated in reference 6. Only one wing size was tested but a range of dynamic pressures from 0.5 to 2.0 pounds per square foot (24.0 to 95.8 N/m^2) was investigated.

Most of the deployments were made on an unslotted wing having the 45° sweep, equal length keel, and leading-edge planform. Two slotted wings having essentially the same planform as the unslotted wing were also tested to see whether a substantial reduction in opening load could be obtained by slotting the wing.

SYMBOLS

The force coefficients are presented with respect to the axis system shown in figure 1. The symbols used in this report are defined as follows:

b_O flat-pattern span, feet (meters)

C_D drag coefficient, $\dfrac{\text{Drag force}}{qS}$ or $-C_X$

C_L lift coefficient, $\dfrac{\text{Lift force}}{qS}$ or $\sqrt{C_Y^2 + C_Z^2}$

C_R resultant-force coefficient, $\dfrac{\text{Resultant force}}{qS}$ or $\sqrt{C_L{}^2 + C_D{}^2}$

C_X normal-force coefficient, $\dfrac{\text{X-axis force}}{qS}$

C_Y axial-force coefficient, $\dfrac{\text{Y-axis force}}{qS}$

C_Z side-force coefficient, $\dfrac{\text{Z-axis force}}{qS}$

l_k keel length, feet   (meters)

m mass, slugs   (kilograms)

q dynamic pressure, pounds/square foot   (newtons/meter^2)

S reference area, 17.29 square feet   (1.606 meters^2)

t time, seconds

t_f canopy filling time, seconds

V velocity along flight path, feet/second   (meters/second)

W weight, pounds   (newtons)

X, Y, Z coordinate axes (see fig. 1)

x_k distance along keel, inches   (meters)

x_{le} distance along leading edge, inches   (meters)

γ flight-path angle, degrees

θ angle of resultant-force vector measured from vertical, degrees (see fig. 1), $\tan^{-1}\dfrac{C_D}{C_L}$

Λ_o flat-pattern leading-edge sweep angle, degrees

ρ air density, slugs/ft^3 (kilograms/meter^3)

MODELS AND APPARATUS

The parawing tested in this investigation was an all-flexible wing having a nominal keel length of 5 feet (1.524 m) and a surface area of 17.29 square feet (1.606 m²). The wing flat pattern and a table giving the location and lengths of the suspension lines are presented in figure 2(a).

The flat-pattern leading-edge sweep of the wing was 45°. The leading edges were equal in length to the keel for the theoretical planform which extended to the pointed apex. The nose section of the canopy, which is one-eighth the keel length, has been cut off, inasmuch as early flight tests showed that when the planform extends to the apex, the nose section has a tendency to collapse. The wing tested had 23 suspension lines, 6 along each leading edge and 11 along the keel. The wing surface was made of acrylic-coated rip-stop nylon fabric weighing 1.1 ounces per square yard (37.2 g/m²) and having nearly zero porosity. The suspension lines were 1/16-inch (0.159 cm) nylon and had a manufacturer's ultimate-strength rating of 100 pounds (444.8 N).

Two slotted wings having essentially the same planform as the basic wing were also tested and are shown in figures 2(b) and 2(c). The wing in figure 2(b) had four over-lapping slots on each panel that ran normal to the center line of each panel and extended from the keel to the leading edge. The wing in figure 2(c) had slots toward the rear and inboard. A small amount of fabric was added to the panel between the slots (see the panel sketch) so that under load the panel would assume a shape like that indicated by section A-A. This wing had 1/2-inch-wide (1.27 cm) cotton tapes stitched to its surface. The tape pattern is indicated by the sketch.

The apparatus used to deploy the wing in the tunnel is shown in figure 3. The wing was attached to a six-component strain-gage balance; the balance was mounted away from the tunnel wall on a three-strut support system. The longitudinal axis of the balance was alined with the tunnel airstream. A cylindrical balance housing with a 5-inch-diameter (12.70 cm) circular plate attached to its base fitted over the end of the balance. A clamp at the center of the circular base plate held the wing suspension lines.

A canister and elastic cord arrangement was used to deploy the wing. The canister was a 5-inch-diameter (12.70 cm), 8-inch-long (20.3 cm) thin-wall metal cylinder. Fastened inside the canister was a cloth deployment bag, about 6 inches (15.23 cm) long and 5 inches (12.70 cm) in diameter. Loops on a flap at the opening of the bag were used for stowing the wing suspension lines. With the wing packed into the deployment bag and the bag fitted inside the canister, the canister was secured to the base plate on the balance. An elastic cord was stretched taut and attached to the canister and to a point downstream. The hooks securing the canister to the mounting plate were designed so that they could be

released from outside the tunnel. These hooks are shown in some detail in the photographs of figure 4. Releasing the hooks allowed the canister to be ejected downstream at a fairly high speed, and the wing deployed. The deployment sequence is shown in figure 5. Loads in the wing suspension lines during opening were transmitted to the balance. The balance readings were obtained on a recording oscillograph.

In some tests the wing was reefed by shortening the sixth keel line back from the nose. A small load cell was added to the reefing line for these tests to measure its tension.

Although the deployment technique simulated somewhat a canister deployment of the type that might be used in a spacecraft recovery system, no attempt was made to simulate a full-scale deployment system, either from the standpoint of the wing and canister weight, the suspension line elasticity, or the canister ejection velocity.

TESTS AND CORRECTIONS

Tests were made at tunnel dynamic pressures of 0.5, 1.0, 1.5, and 2.0 pounds per square foot (24.0, 47.9, 71.8, and 95.8 N/m^2). Several deployments were made at each dynamic pressure. For sea-level conditions the wind velocities corresponding to these dynamic pressures are 20.5, 29.0, 35.5, and 41.0 feet per second (6.25, 8.85, 10.80, and 12.50 m/sec), respectively. The Reynolds number, based on the model keel length of 5 feet (1.524 m), varied from about 6.5×10^5 at the lowest test velocity to about 1.30×10^6 at the highest test velocity.

In most tests the deployment canister was used to deploy the wing. However, in some cases the wing was folded in an accordion fold from nose to trailing edge and then held by hand, until the tunnel was brought up to speed, and then released. In either packing or holding the wing, the nose section was positioned such that when the wing was deployed, it rotated sideways toward the center of the tunnel and away from the tunnel wall.

No blockage or jet boundary corrections were applied to the data. Blockage effects were minimized by having a model that was small compared with the test section. (The ratio of model wing area to test-section cross-sectional area was about 0.06.)

The oscillograph record shown in figure 6(a) is typical of the records obtained during the tunnel deployments of the unreefed configuration. The record shows X-, Y-, and Z-axis force traces from the time just before release of the deployment canister until the wing had reached its trim point and assumed a steady-state flying attitude in the tunnel. The large drop in axial force shortly after the record was started indicates the release of the deployment canister. The snatch load (the load at the time of line stretch)

is indicated by a small axial-force pulse that occurred just before the start of wing fill. The secondary oscillation that appeared on the records, most noticeable on the side-force trace, was caused by an oscillation in the strut support system. Lift- and drag-coefficient data were obtained from the records by resolving the two components of force normal to the airstream into lift, and, of course, the axial-force component becomes drag.

Figure 6(b) shows a typical oscillograph record obtained during tests of the reefed wing. At the time these tests were made, only the axial component of the balance force was being recorded. Figure 6(b) shows the axial-force trace plus the readings from the small load cell located in the reefing line.

RESULTS AND DISCUSSION

Wind-Tunnel Results for the Basic Unslotted Wing

Results of the wind-tunnel deployments of the basic unslotted wing are presented in figures 7(a) to 9(b). Figures 7(a) to 7(d) show lift- and drag-coefficient time histories obtained from two separate deployments at dynamic pressures from 0.5 to 2.0 pounds per square foot (24.0 to 95.8 N/m^2), respectively. The magnitude and direction of the resultant force vector is shown by the vector plot at the right (for the first deployment only). Canopy filling time is plotted against tunnel dynamic pressure in figure 8. Filling time was measured from figures 7(a) to 7(d) as the time from start of opening to the time the wing developed its maximum resultant force, since the tests were made under infinite-mass conditions (no decrease in velocity during opening) and the wing therefore develops its maximum force at the moment it attains maximum area. Figures 9(a) and 9(b) show the force time history nondimensionalized with respect to filling time. The data in figures 9(a) and 9(b) are the same data as presented in figures 7(a) to 7(d) except that the force is presented in terms of its magnitude C_R (fig. 9(a)) and inclination θ (fig. 9(b)), and is plotted against the nondimensional time parameter t/t_f.

The results indicate that the problem of calculating the opening shock for the para-wing involves solving the two-degree-of-freedom equations of motion and not the single-degree-of-freedom equation required in parachute analysis, since there is a buildup in both lift and drag coefficient to very large values during the opening process. The wing began to develop lift almost as soon as it started to open. It began to rotate about its suspension-line confluence point after it had unfolded until it reached its trim angle of attack. At that point it performed a slight oscillation before steadying out.

The maximum lift and drag coefficients developed during opening were both about 2.5. The steady-state lift and drag coefficients were about 1.05 and 0.55, respectively; these values are consistent with the static force-test results presented in references 3

6

and 4. The shock factor — the ratio of maximum resultant-force coefficient to steady-state resultant-force coefficient — was about 3.0. The resultant-force vector was inclined about 48° to the airstream when the wing developed its maximum force.

Filling times obtained from figure 7, as the time from the start of opening to the time of maximum force, are plotted against tunnel dynamic pressure in figure 8. For wind-tunnel deployments of parachutes, the filling time is usually found to be directly proportional to the size of the parachute and inversely proportional to the deployment velocity. By assuming that this relationship holds true for the parawing also, an empirical formula for filling time was derived from the results of the present tests, as shown by the dashed line in figure 8. The formula $t_f = 2.5 \frac{l_k}{V}$ is shown in figure 8 to give a good approximation of the filling time of the 5-foot (1.524 m) parawing over the complete range of test dynamic pressures. The filling times given by this equation, however, are those for infinite-mass conditions (that is, where the velocity remains constant all during the deployment). The equation could not necessarily be used to predict filling times for actual flight (finite-mass) deployments where there is a large drop in the free-stream velocity during the deployments.

Perhaps, equally as important as filling time in making opening-shock calculations for parawings or parachutes for actual flight conditions is the filling distance — the distance traveled from the start of opening to the time complete inflation has occurred. According to reference 7, this distance is always the same for a parachute of a given size and design, regardless of the altitude or velocity at which the parachute begins to open. It, therefore, may be one of the fundamental parameters to be considered in the parachute or parawing opening process. A first approximation to the filling distance of the parawing was obtained from the results of the present investigation. The test results indicate that the filling distance for the parawing design tested is $2.5 l_k$.

Figure 9 shows that the force time history could be nondimensionalized to a satisfactory degree by plotting against the time parameter t/t_f. All the data of figures 7(a) to 7(d) are seen to combine into two curves, one for θ and the other for C_R. There is some scatter in values of C_R and θ at values of t/t_f below 1.6 and especially around C_R maximum. (Scatter in values of θ could be attributed to some extent to the inaccuracies of θ determined from small lift and drag readings.) Curves of θ as a function of t/t_f are also seen to diverge from one another at values of t/t_f above 1.6, where the wing tended to oscillate before steadying out to its trim angle of attack. The oscillation had a higher amplitude at the higher dynamic pressures. The two faired curves, however, give a fairly accurate representation for the complete time history from the start of opening to the time steady-state conditions are reached. Values of C_R and θ taken from figure 9 and listed in table I were the ones used in the digital computer calculations made in this report.

Comparison of Wind-Tunnel Results With Model Flight-Test Results

for the Basic Unslotted Wing

To indicate the accuracy of the wind-tunnel data in comparison with actual flight-test results, opening forces for a 5-foot (1.524 m) all-flexible parawing model were calculated by using the wind-tunnel data and the results were compared with drop-test results for the model. The drop tests were made from a 100-foot (30.48 m) tower. The wing was identical to the wing deployed in the tunnel tests except that it had a scaled Apollo command module attached to its suspension lines. The capsule was instrumented with a single load cell which measured total load in the suspension lines. The loads were recorded by extending a lightweight wire from the load cell to a recording oscillograph on the ground. The model wing loading was varied from 0.19 to 0.97 pound per square foot (9.10 to 46.40 N/m^2) by adding weights to the capsule. The wing was folded and packed using the same procedure and same size deployment bag as those used in the wind-tunnel tests and was deployed with a 30-foot (9.14 m) static line. The velocity at the start of wing opening was determined to be about 52.0 feet per second (15.8 m/sec) (q = 3.2 pounds per square foot or 153.2 N/m^2) from motion pictures taken of the drop.

The opening-force calculations were made on a digital computer by use of data obtained from figure 9 and listed in table I. The computer solved the two-degree-of-freedom point-mass equations of motion, which are:

$$m \frac{dV}{dt} = -\rho \frac{V^2 S C_D}{2} - W \sin \gamma$$

along the flight path and

$$mV \frac{d\gamma}{dt} = \rho \frac{V^2 S C_L}{2} - W \cos \gamma$$

normal to the flight path.

The data in table I are listed as a function of t/t_f but were fed into the computer program as a function of real time which was obtained by multiplying t/t_f by the value of t_f for the calculations. The filling time used (t_f = 0.24 sec) was that for infinite-mass conditions for the 5-foot (1.524 m) wing at a velocity of 52.0 feet per second (15.8 m/sec). The comparison presented in figure 10 shows good agreement between the calculated and measured force time histories. As is typical of deployments under finite-mass conditions, maximum force did not occur at t = 0.24 second when the wing was fully open, because of the decrease in dynamic pressure occurring as the wing opens. The computer calculations did not account for the low level of force obtained after the wing had experienced maximum opening force, nor were the calculations able to predict

very accurately the initial rate of change of opening force. The calculated results did, however, give an accurate prediction of the maximum opening force for all three wing loadings.

Wind-Tunnel Results for Slotted Wings

Time histories of lift and drag coefficient and vector plots for the two slotted wings are presented in figures 11(a) and 11(b). Figure 11(a) gives the results for the wing which had four overlapping slots on each panel shown in figure 2(b). Figure 11(b) gives results for the wing shown in figure 2(c). The results for both slotted wings, which were obtained at $q = 1.0$, were very similar to the results for the basic unslotted wing at $q = 1.0$. (See fig. 7(b).) The time rate of load buildup was about the same and there was no noticeable difference in filling time. The wing with slotted panels toward the rear and inboard gave slightly lower maximum lift and drag coefficients than either the unslotted or the other slotted wing, but its steady-state lift and drag coefficients were also lower. The shock factor was about the same for all three wings.

Subsequent to the completion of the present wind-tunnel deployment tests, free-flight deployment loads measured on a multiple slotted wing having an area of about 400 square feet (37.16 m^2) indicated a significantly lower opening shock for the slotted wing than for a comparable unslotted wing. Both the planform and slot configuration were different from the slotted wings used in the wind-tunnel tests reported herein.

Reefing

Limited tests were also made of a reefing technique in which opening load reduction was attempted by shortening one of the suspension lines attached to the keel — the sixth line back from the nose. This shortening has the effect of putting a large spanwise crease in the wing at the point where the suspension line was attached to the wing and resulted in a shorter chord configuration. It is similar to the method used on parachutes of pulling down on a line attached to the center of the canopy and has the advantage of being fairly simple in operation and provides variable reefing. It has the disadvantage of possibly causing high loads in the reefing line plus the possibility of canopy inversion under high loading conditions. At the time these tests were made, only one component of opening force, the axial force, was being recorded. Drag data, therefore, are the only data available for making a comparison between reefed and unreefed loads, but these data should give a fairly good indication of the effectiveness of the reefing technique in reducing loads. The comparison of time histories for reefed wing and for various amounts of shortening of the reefing line is presented in figure 12. Results of the reefing tests are summarized in figure 13 which shows a maximum drag coefficient and the maximum reefing line load coefficient obtained during opening as a function of reefing line shortening. These data

show that reefing produced a substantial reduction in maximum drag coefficient. Drag coefficient was reduced from its unreefed value of about 2.4 to about 1.4 with the reefing line shortened 5.9 percent and to about 0.6 with the reefing line shortened 11.8 percent. There was no large increase in the reefing line load.

CONCLUSIONS

A study of the opening forces of an all-flexible parawing having a keel length of 5 feet (1.524 m), a flat-planform leading-edge sweep of 45°, and equal-length leading edges and keel indicated the following conclusions:

1. The resultant-force coefficient reached a maximum value of about 3.0 times its steady-state value when it was inclined about 48° from the direction of flow. The problem of calculating opening shock for the all-flexible parawing involves solving the two-degree-of-freedom equations of motion, since there is a large buildup in both lift and drag during opening. Lift and drag coefficients both reached maximum values of about 2.5 during opening.

2. Canopy filling time t_f for infinite-mass conditions could be approximated by the equation $t_f = 2.5 \frac{l_k}{V}$ where l_k is the keel length and V is the velocity. The opening-force time history could be nondimensionalized to a satisfactory degree by plotting against the ratio of real time to filling time.

3. Opening-force time histories for a 5-foot (1.524 m) all-flexible parawing dropped from a tower could be estimated by using the wind-tunnel data.

4. The two slotted wings investigated in the wind-tunnel deployments gave no noticeable reduction in the opening force; however, flight tests of another slotted configuration indicated an appreciable reduction in opening shock.

5. Reefing by pulling in on one of the suspension lines attached to the keel reduced the opening drag force.

Langley Research Center,
    National Aeronautics and Space Administration,
        Langley Station, Hampton, Va., November 20, 1968,
           124-07-03-22-23.

REFERENCES

1. Naeseth, Rodger L.; and Gainer, Thomas G.: Low-Speed Investigation of the Effects of Wing Sweep on the Aerodynamic Characteristics of Parawings Having Equal-Length Leading Edges and Keel. NASA TN D-1957, 1963.

2. Croom, Delwin R.; Naeseth, Rodger L.; and Sleeman, William C., Jr.: Effects of Canopy Shape on Low-Speed Aerodynamic Characteristics of a 55° Swept Parawing With Large-Diameter Leading Edges. NASA TN D-2551, 1964.

3. Libbey, Charles E.; Ware, George M.; and Naeseth, Rodger L.: Wind-Tunnel Investigation of the Static Aerodynamic Characteristics of an 18-Foot (5.49-Meter) All-Flexible Parawing. NASA TN D-3856, 1967.

4. Naeseth, Rodger L.; and Fournier, Paul G.: Low-Speed Wind-Tunnel Investigation of Tension-Structure Parawings. NASA TN D-3940, 1967.

5. Hamilton, J. Scott: Flight of the Parawing. Parachutist, vol. 7, no. 9, Sept. 1966, pp. 5-9.

6. Waters, M. H. L.: Elementary Estimates of Parachute Opening Forces. Tech. Note Mech. Eng. 238, Brit. R.A.E., May 1957.

7. French, Kenneth E.: Inflation of a Parachute. AIAA J., vol. I, no. 11, Nov. 1963, pp. 2615-2617.

TABLE I

WIND-TUNNEL DATA USED IN OPENING-FORCE CALCULATIONS

t/t_f	c_R	θ, deg	c_L	c_D
0	0	90.0	0	0
.2	.23	86.3	.0149	.228
.4	.75	81.5	.109	.741
.6	1.57	74.6	.417	1.512
.8	2.62	63.3	1.177	2.34
1.0	3.00	41.8	2.24	2.00
1.2	1.83	24.3	1.667	.753
1.4	.92	17.4	.878	.275
1.6	.66	18.0	.627	.204
1.8	.72	22.3	.665	.273
2.0	.91	26.3	.815	.403
2.2	1.07	29.7	.933	.532
2.4	1.23	32.0	1.042	.651
2.6	1.37	33.3	1.143	.752
2.8	1.43	33.8	1.189	.796
3.0	1.30	32.3	1.100	.695
3.2	1.10	29.1	.960	.535
3.4	.99	25.9	.891	.433
3.6	.95	24.0	.867	.386
3.8	.95	24.1	.866	.388
4.0	.96	25.1	.860	.403
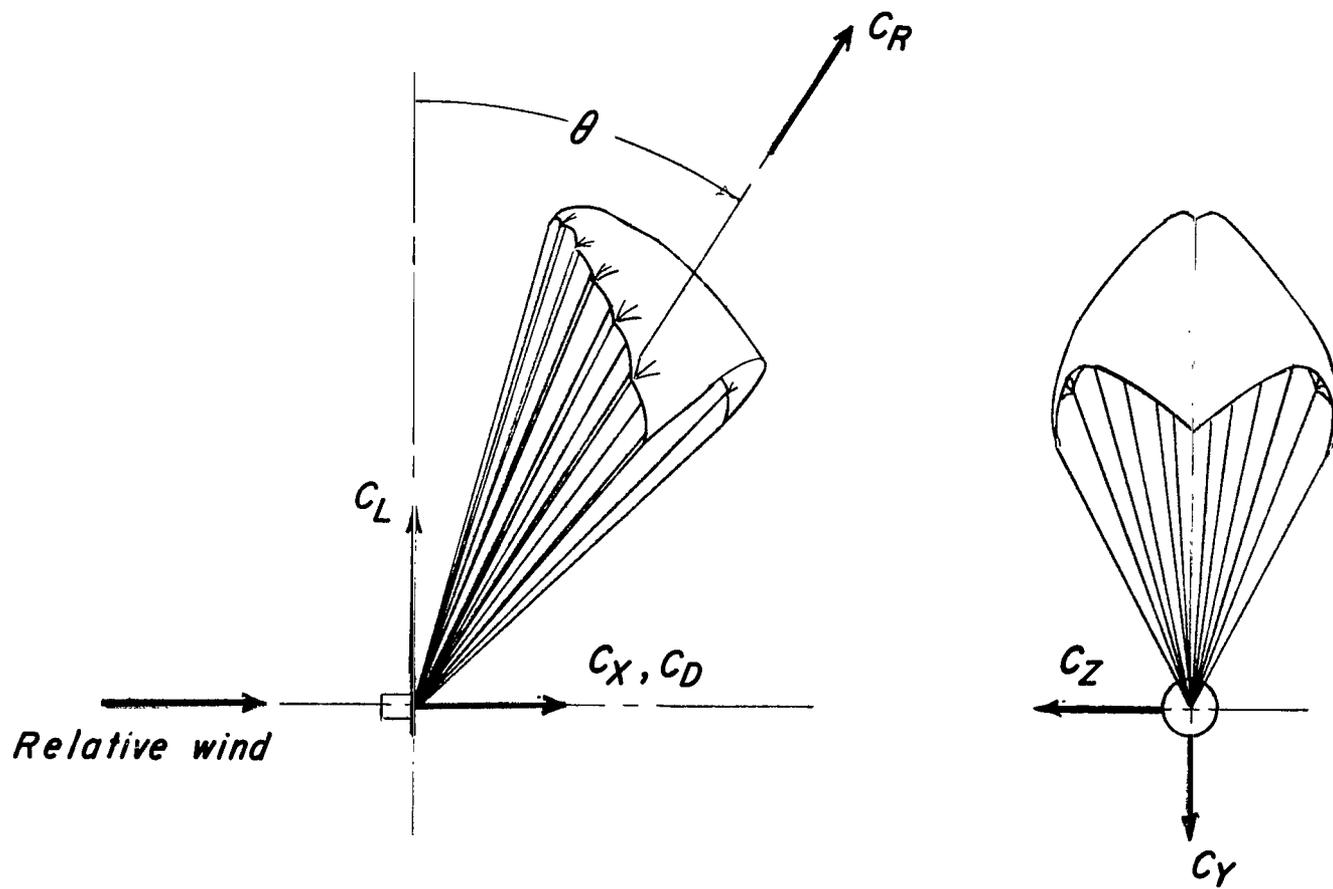
Figure 1.- Axes system showing positive direction of forces.
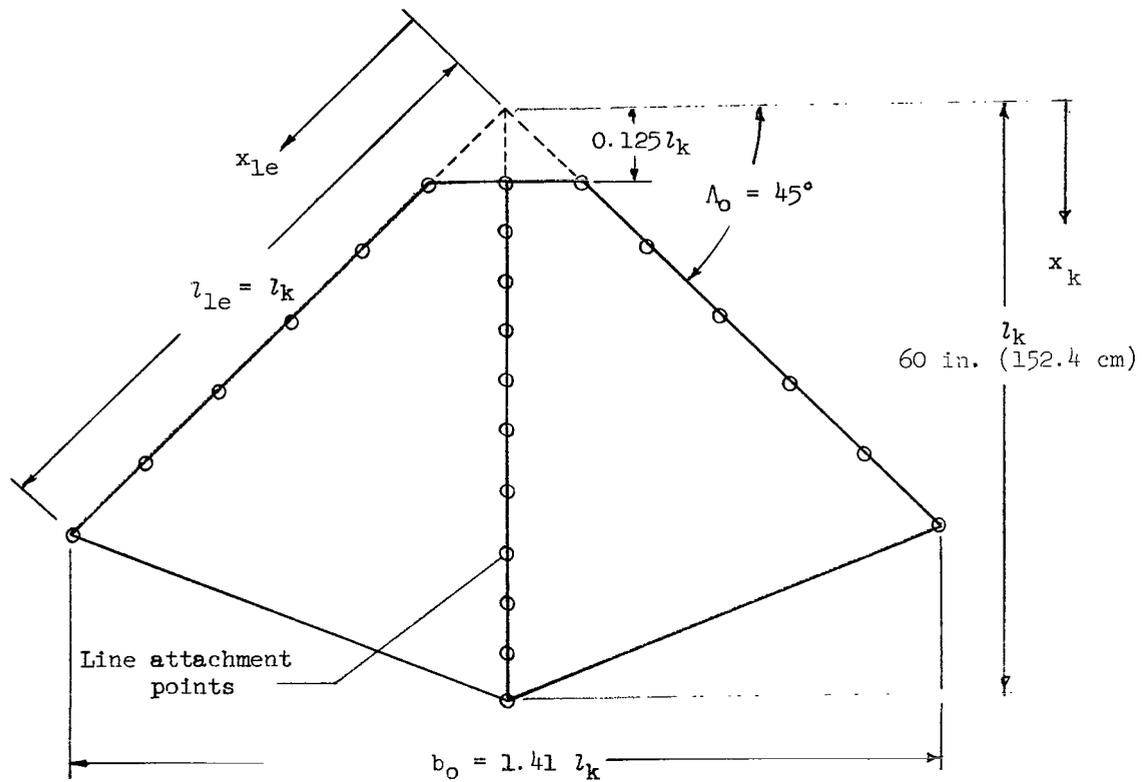
Shroud Line Locations and Lengths

Keel			Leading edges		
x_k/l_k	Line length, in.	Line length, cm	x_{le}/l_k	Line length, in.	Line length, cm
0.125	79.50	201.93	0.177	79.75	202.57
.208	79.13	200.98	.333	76.50	194.31
.292	79.13	200.98	.500	74.25	188.60
.375	78.25	198.76	.667	70.00	177.80
.459	76.75	194.95	.833	67.13	170.50
.542	76.25	193.68	1.000	61.25	155.58
.645	76.25	193.68			
.750	76.25	193.68			
.833	75.88	192.72			
.917	72.25	183.51			
1.000	68.50	173.99			

(a) Basic unslotted wing.

Figure 2.- Sketches of flat patterns of parawings tested.
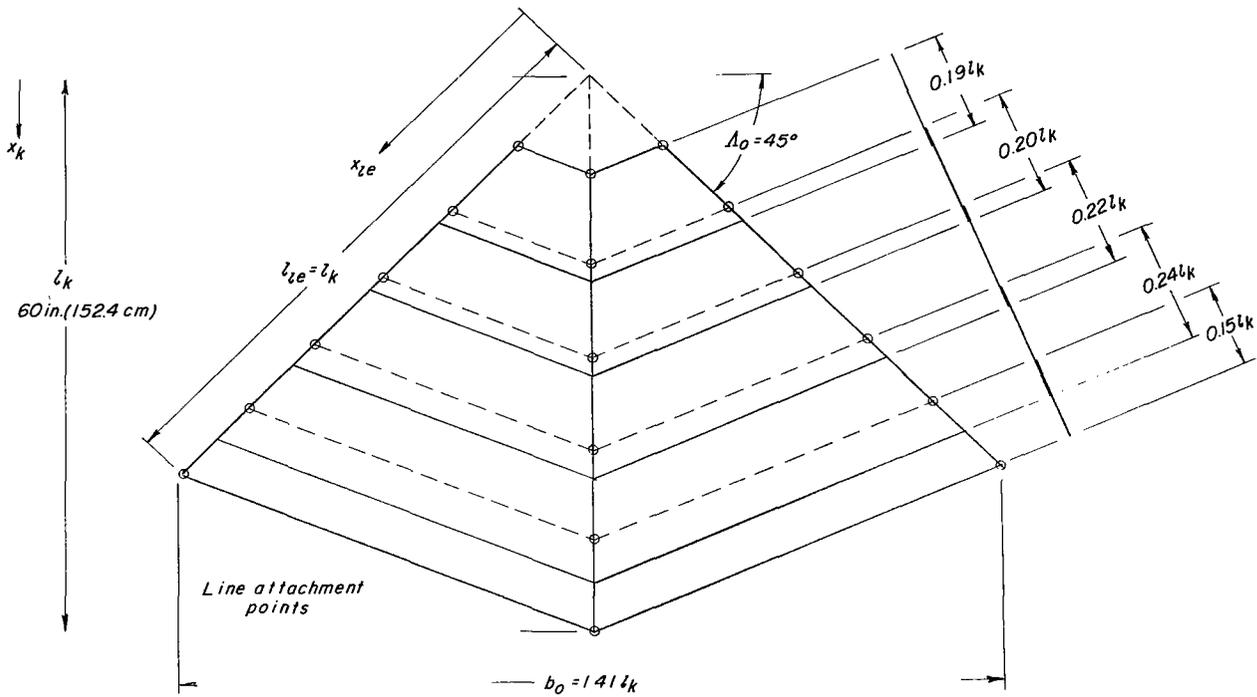
x_k/l_k	x_{le}/l_k
.167	.167
.333	.333
.500	.500
.667	.667
.833	.833
1.000	1.000

Line attachment location

(b) Wing with overlapping slots.

Figure 2.- Continued.

0.125 l_k

$\Lambda_0 = 45°$

x_{le}

$l_{le} = l_k$

.008 l_k cotton tape

x_k

22.5°

l_k

60 in. (152.40 cm)

Line attachment
points

Slot panels

$b_o = 1.414 l_k$

Section A-A

5°

5°
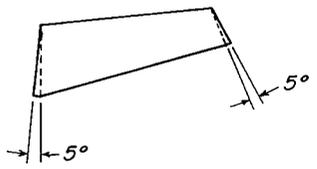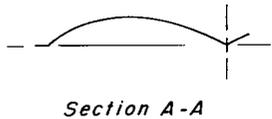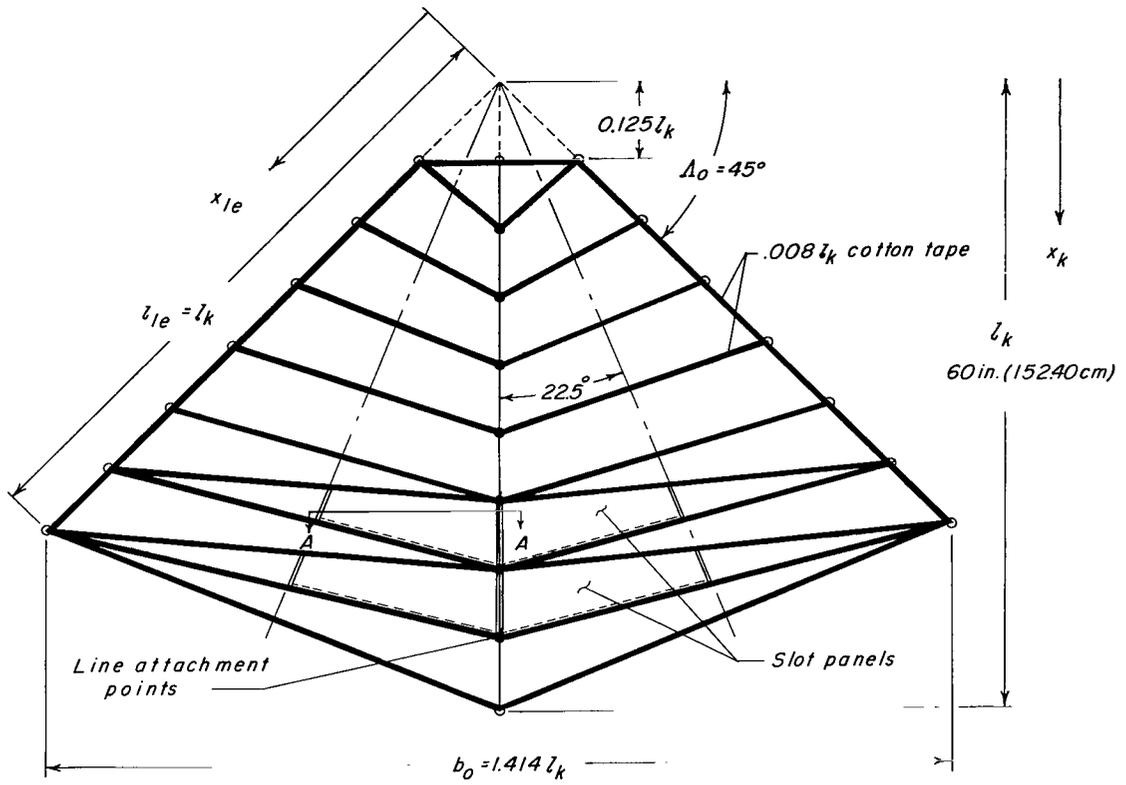
Typical slot panel, note excess of 5° at
each end to give fullness.

x_k/l_k	x_{le}/l_k
.125	.177
.233	.314
.342	.452
.450	.588
.558	.726
.667	.863
.775	1.000
.883	
1.000	

Line attachment location

(c) Wing with slots located toward the rear and inboard.

Figure 2.- Concluded.

Tunnel wall

Support struts

Relative wind

Base plate

Six-component
strain-gage balance

Balance housing

Canister containing cloth
packing bag and parawing

Restraining lines

3.8 ft

8.5 ft
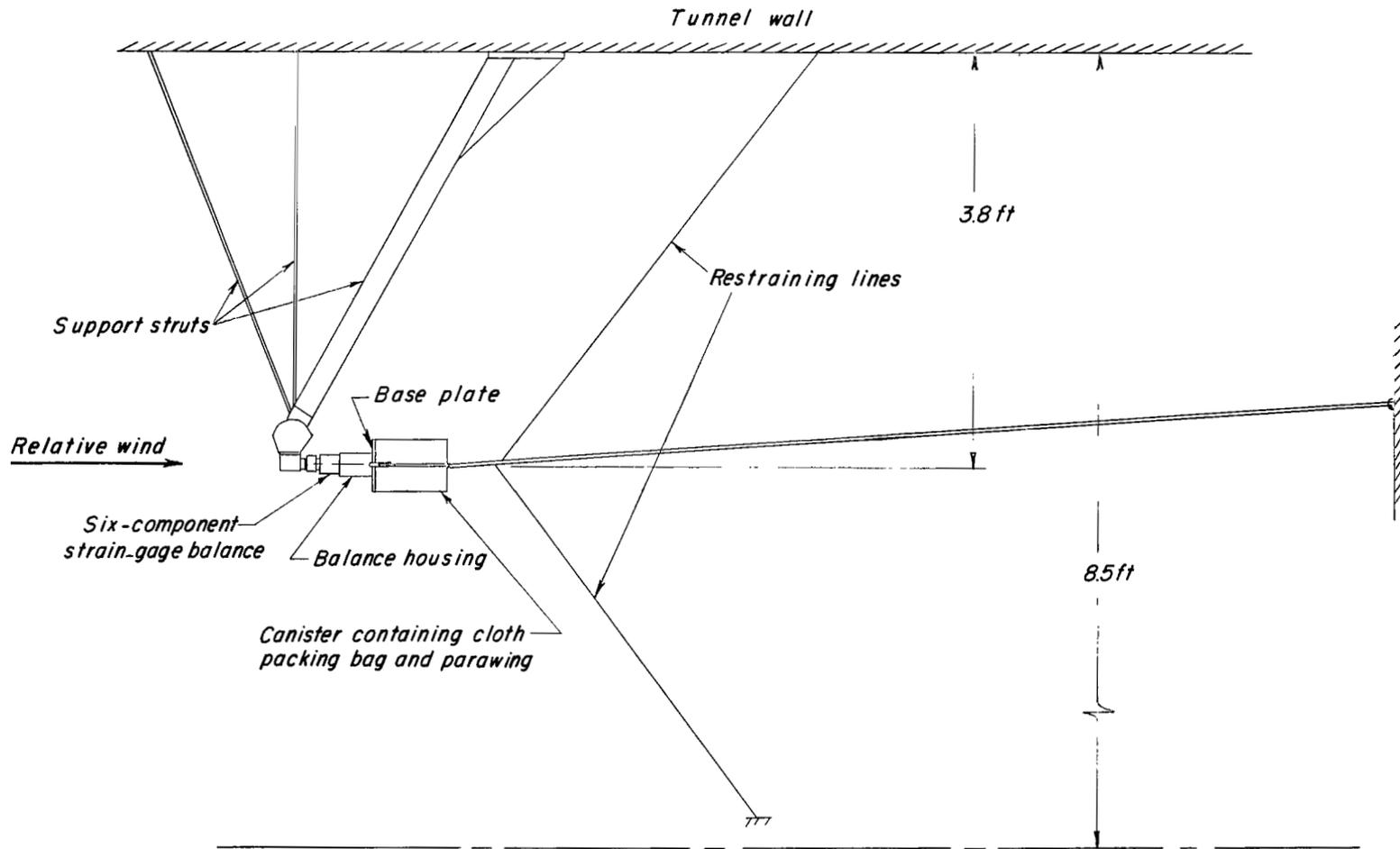
Figure 3.- Sketch of test installation.

Release hooks

Suspension-line clamp

Lines for hooking to base plate

Balance housing and base plate
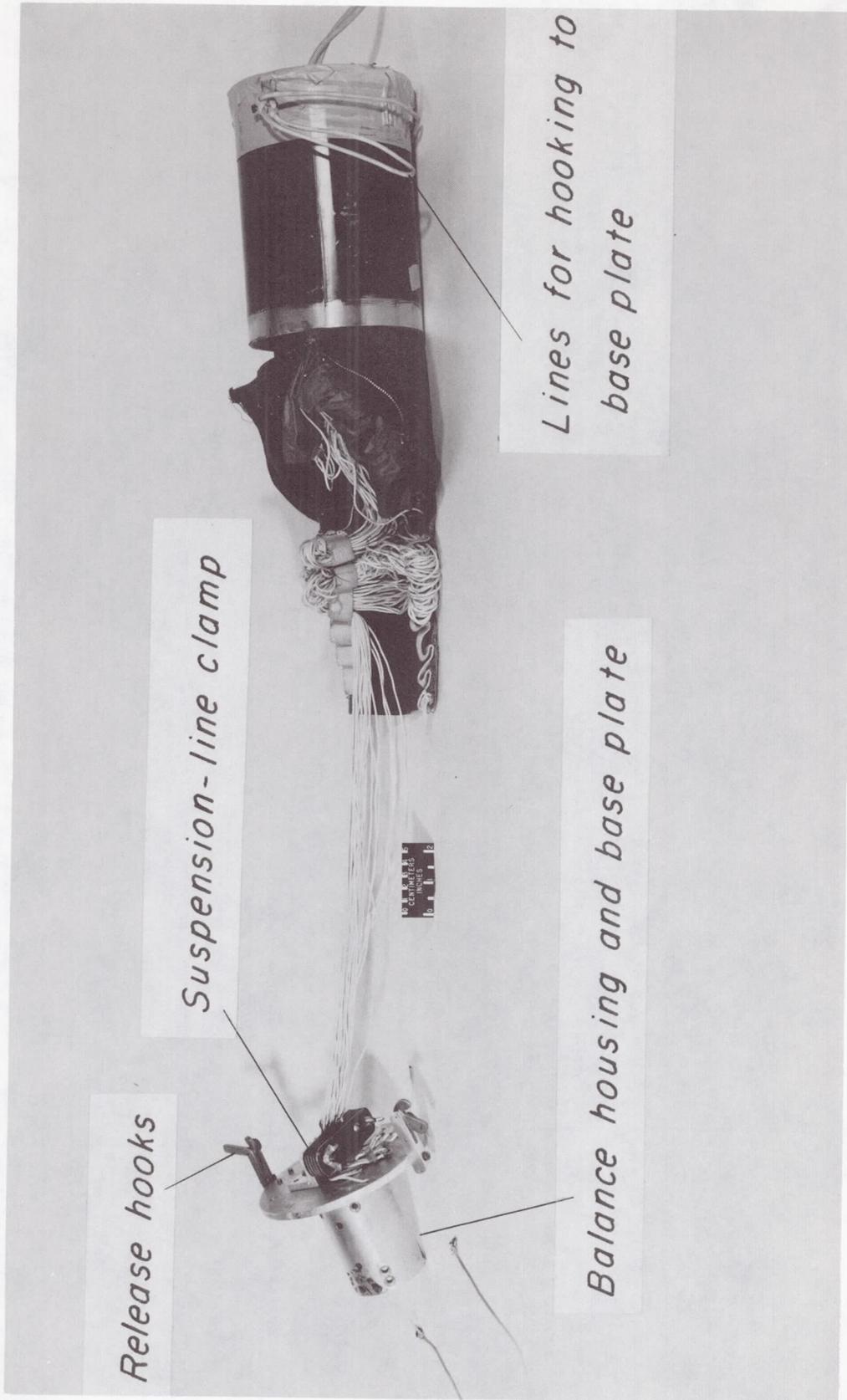
Figure 4.– Photograph showing arrangement of balance housing, deployment canister, and parawing.

18
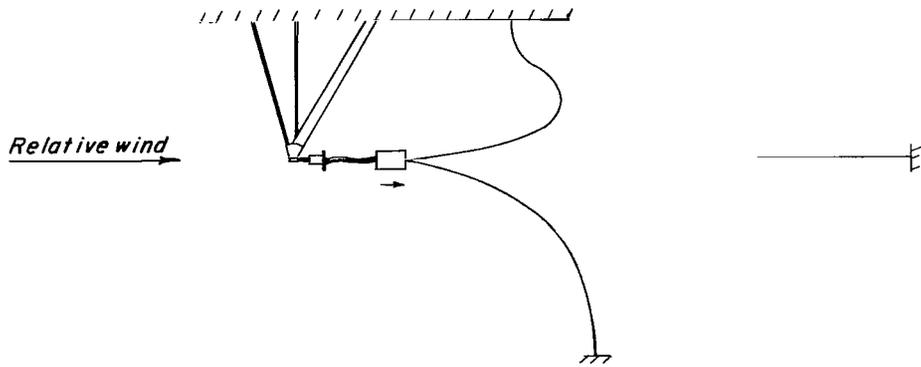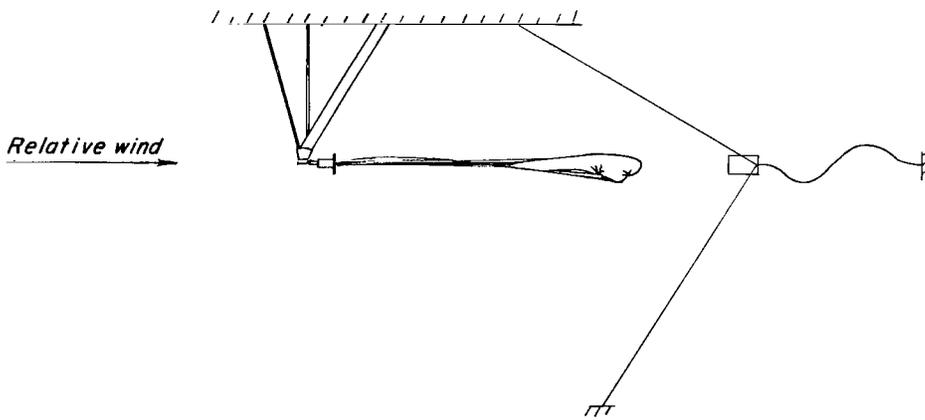
(a) Deployment.

(b) Wing emerged from canister; opening starts.
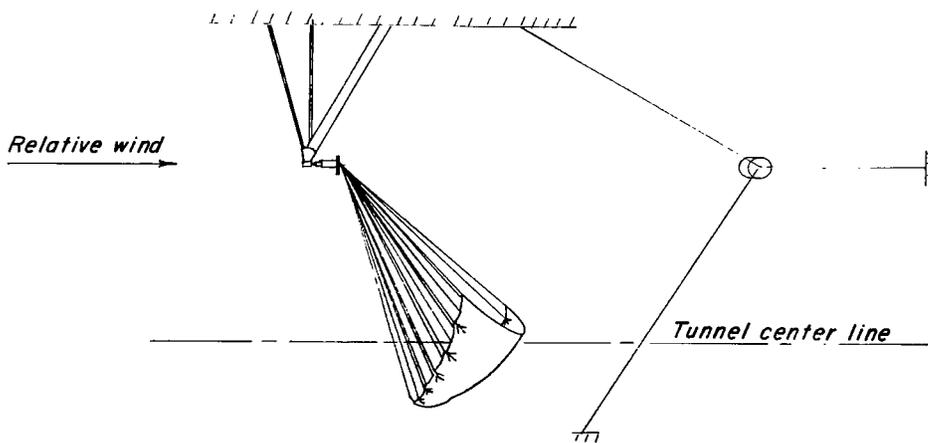
(c) Wing in steady-state attitude.

Figure 5.- Sequence of events during deployment.

19
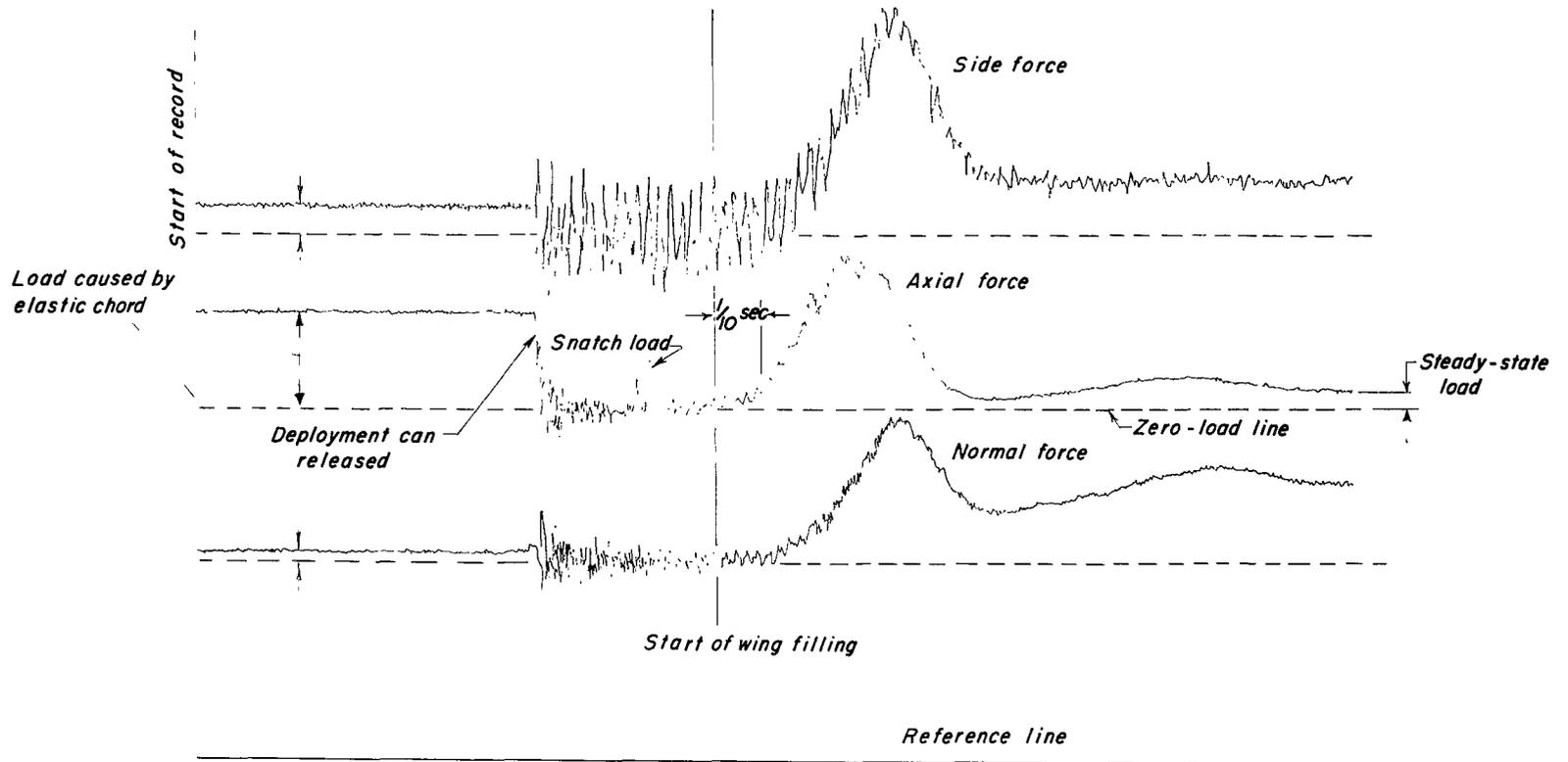
(a) Normal-, axial-, and side-force traces for test of basic unslotted wing.

Figure 6.- Typical oscillograph records.

Dynamic pressure = 20 lb/ft² (95.8 N/m²)
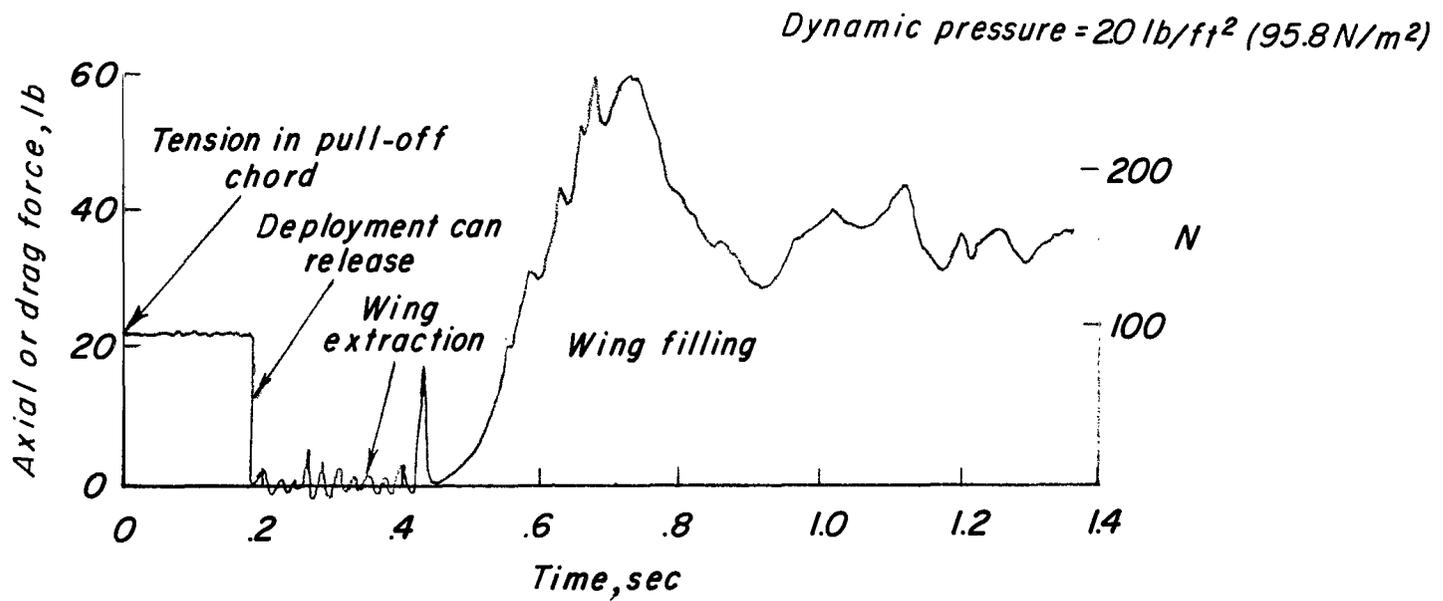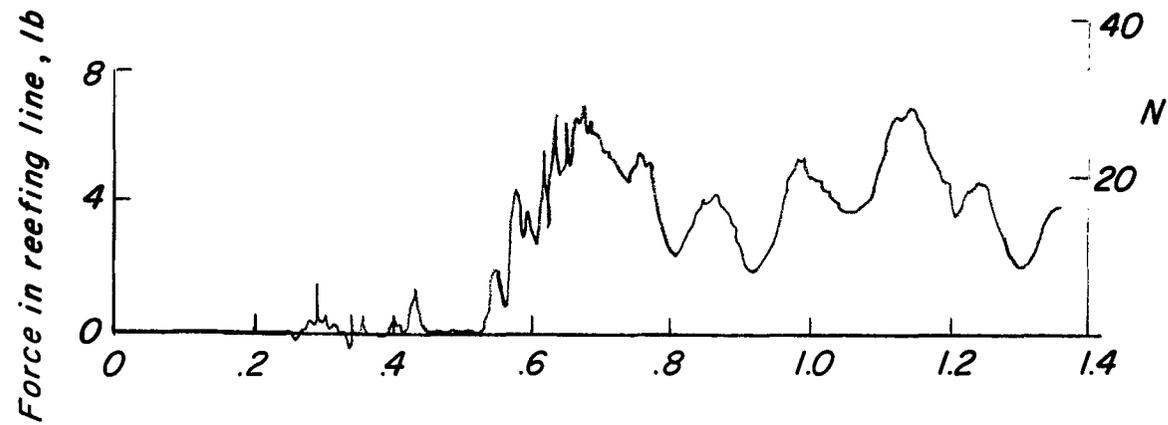
(b) Typical time histories of total deployment load and load in reefing line.

Figure 6.- Concluded.

1st deployment
-----2nd deployment
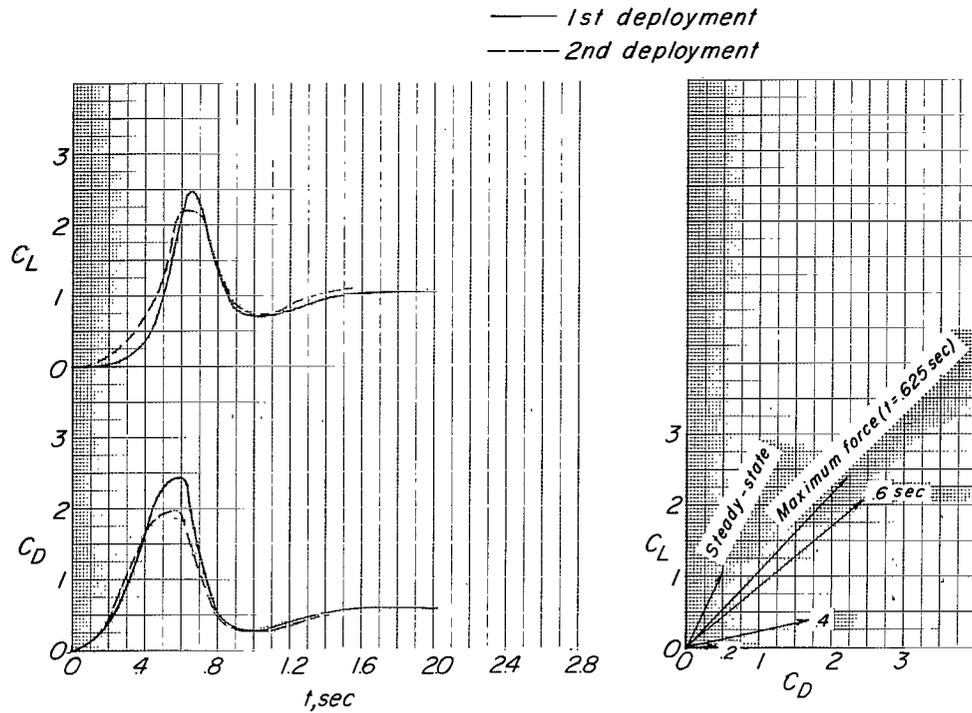
(a)   q = 0.5 lb/ft^2 (24.0 N/m^2).
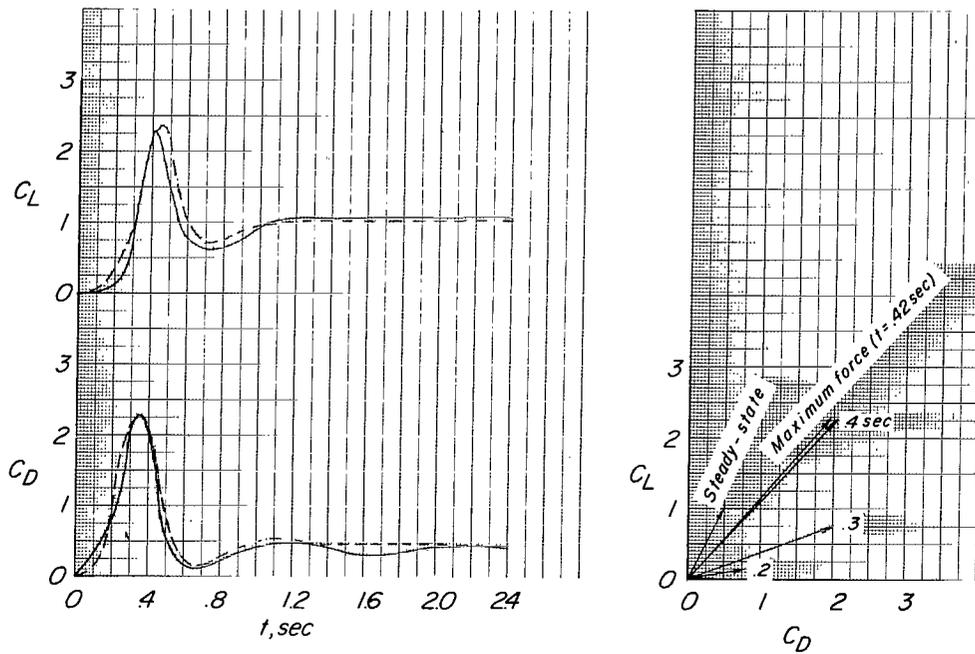
(b)   q = 1.0 lb/ft^2 (47.9 N/m^2).

Figure 7.- Time histories of lift and drag coefficient for the basic unslotted wing.

——— *1st deployment*

– – –*2nd deployment*
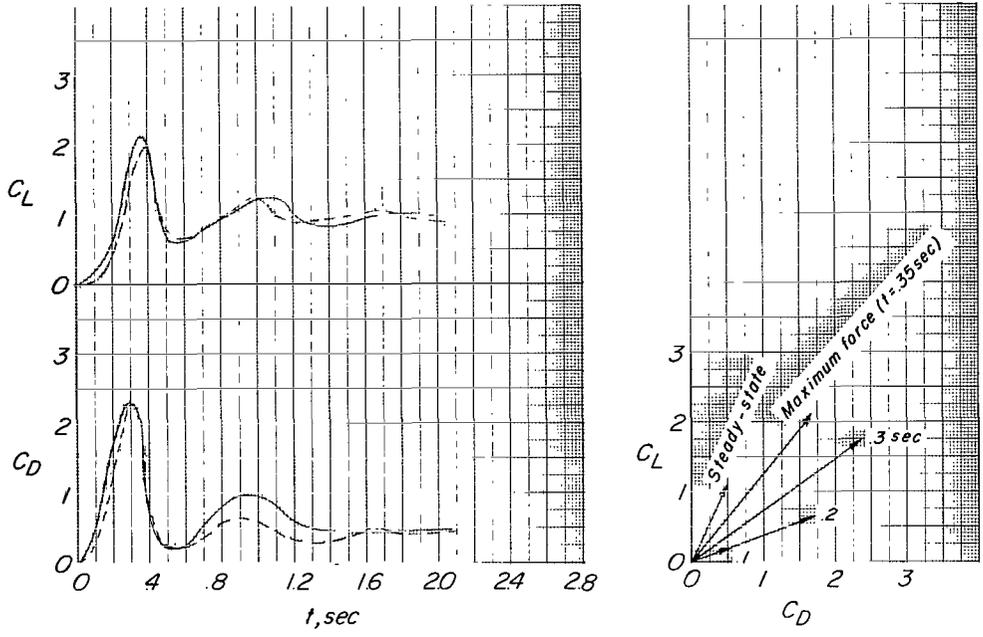
(c) q = 1.5 lb/ft^2 (71.8 N/m^2).
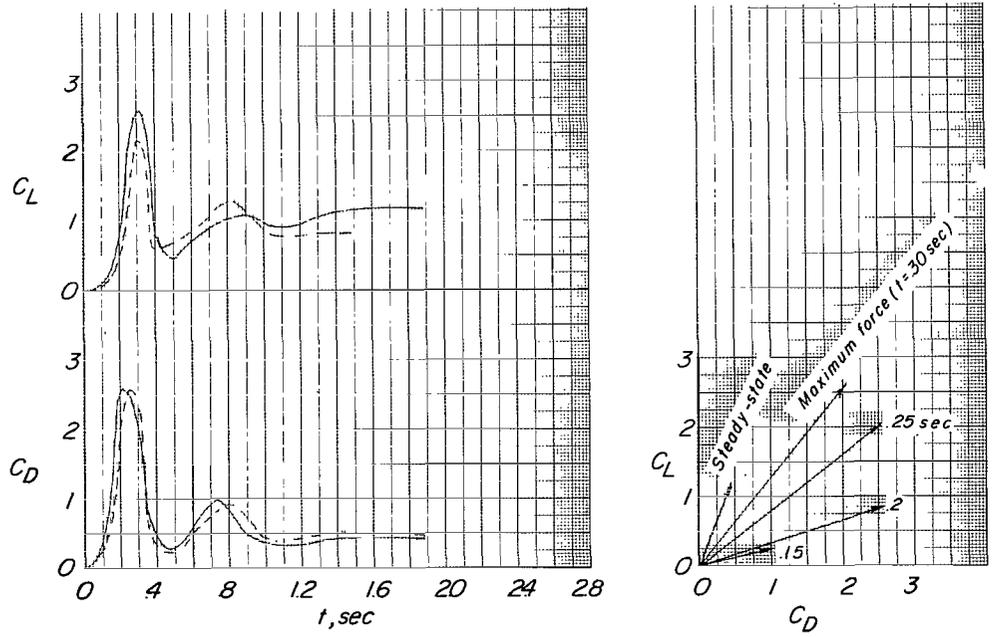
(d) q = 2.0 lb/ft^2 (95.8 N/m^2).

Figure 7.- Concluded.
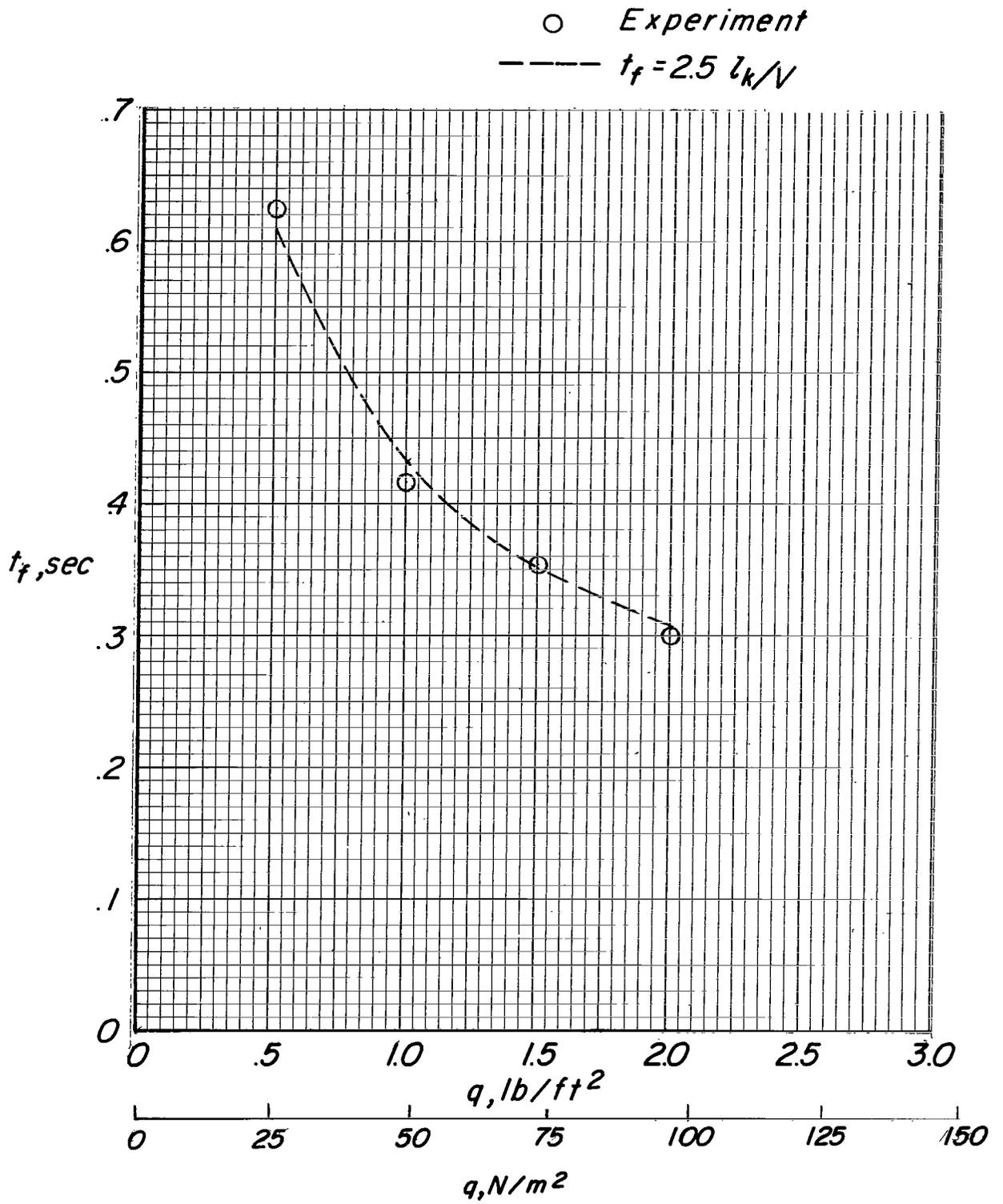
Figure 8.- Variation of canopy inflation time with wind-tunnel dynamic pressure.

24

q, N/m²	q, lb/ft²
24	.5
47.9	1.0
71.8	1.5
95.8	2.0

Unflagged symbols are for 1st deployment

Flagged symbols are for 2nd deployment
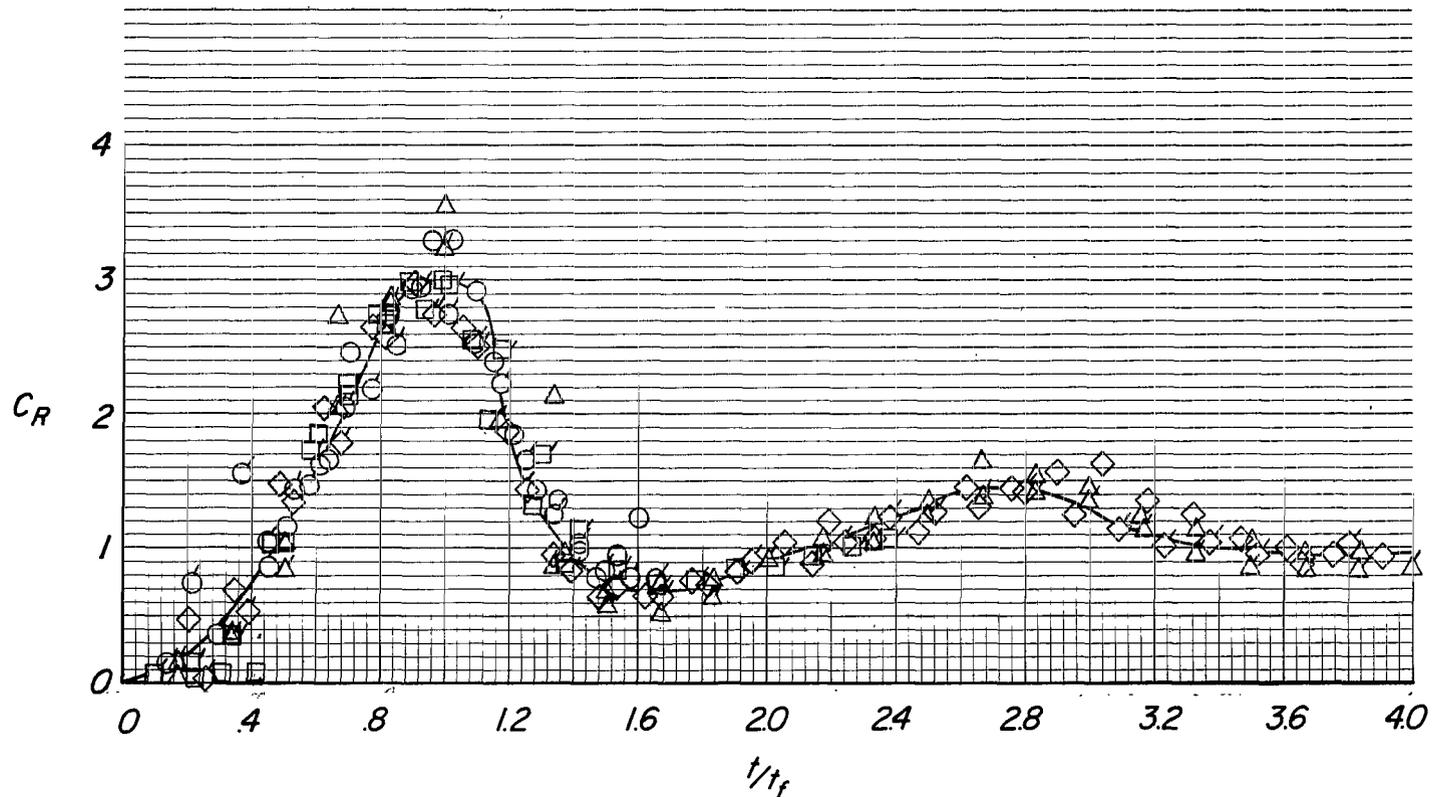
(a) Resultant-force coefficient.

Figure 9.- Nondimensionalized plots of magnitude and inclination of resultant-force vector during wing opening.
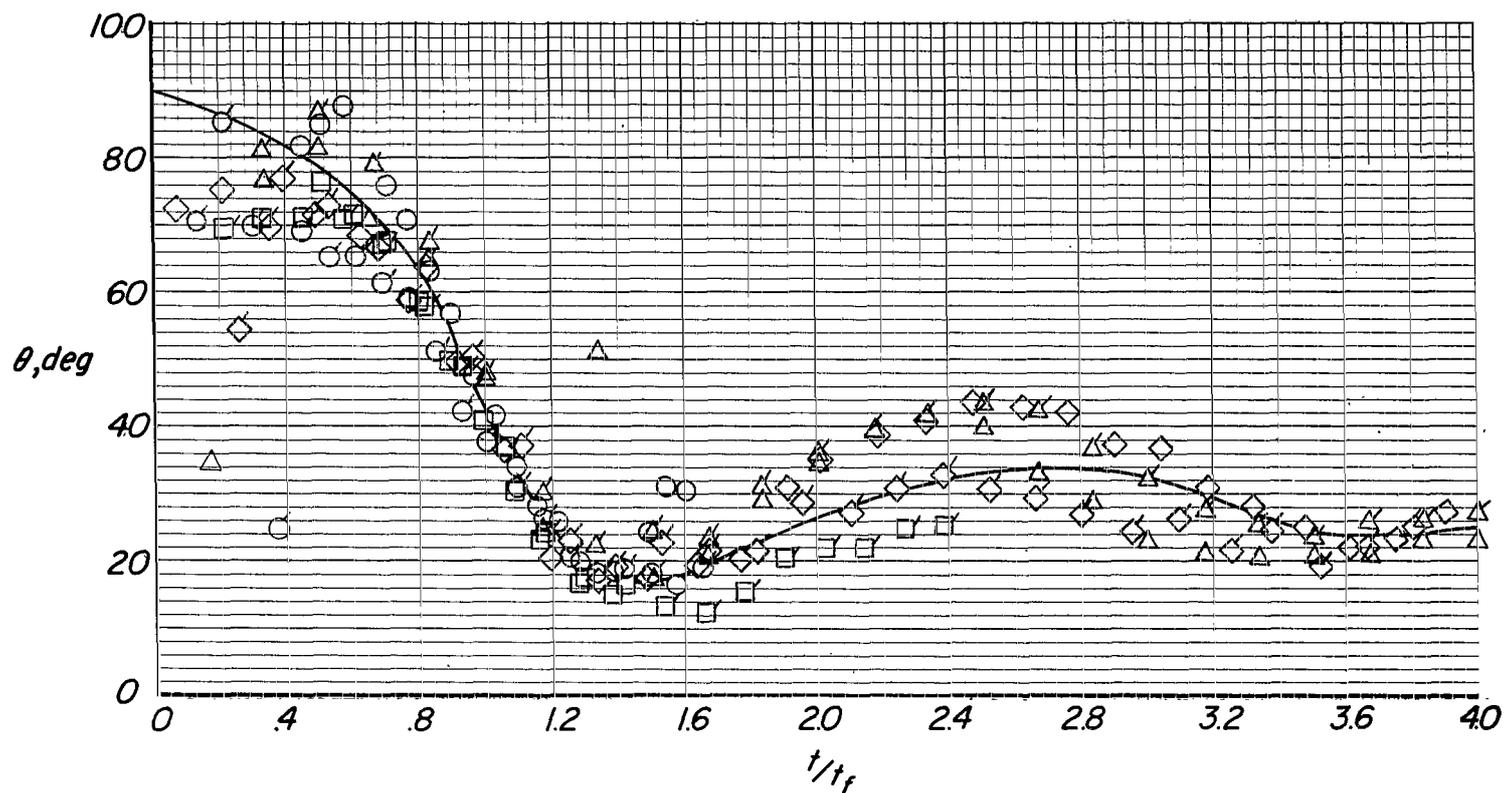
(b) Angle of inclination of resultant-force vector.

Figure 9.- Concluded.
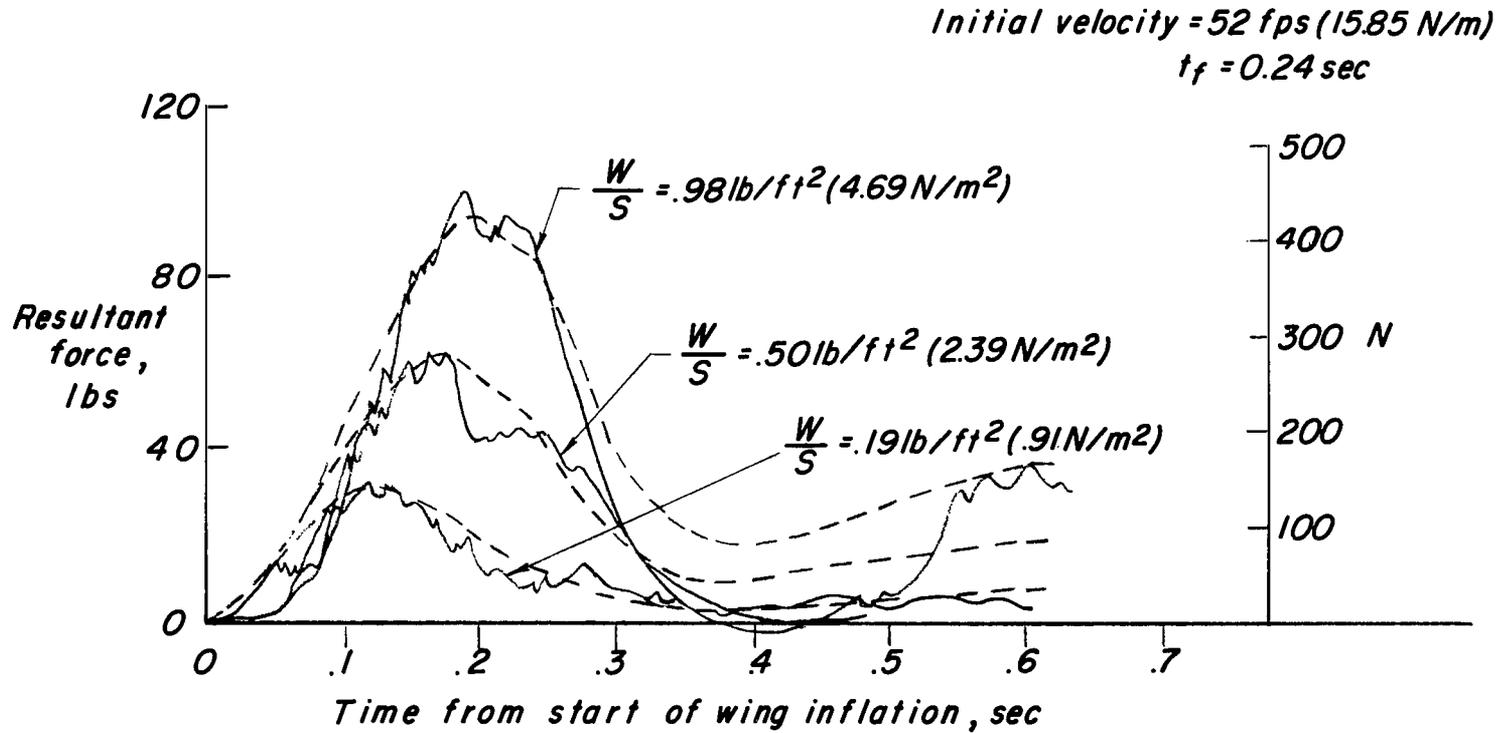
Figure 10.- Comparison of calculated and measured opening-load time histories for a 5-foot (1.523-m) all-flexible parawing space-capsule combination during free-drop tests.
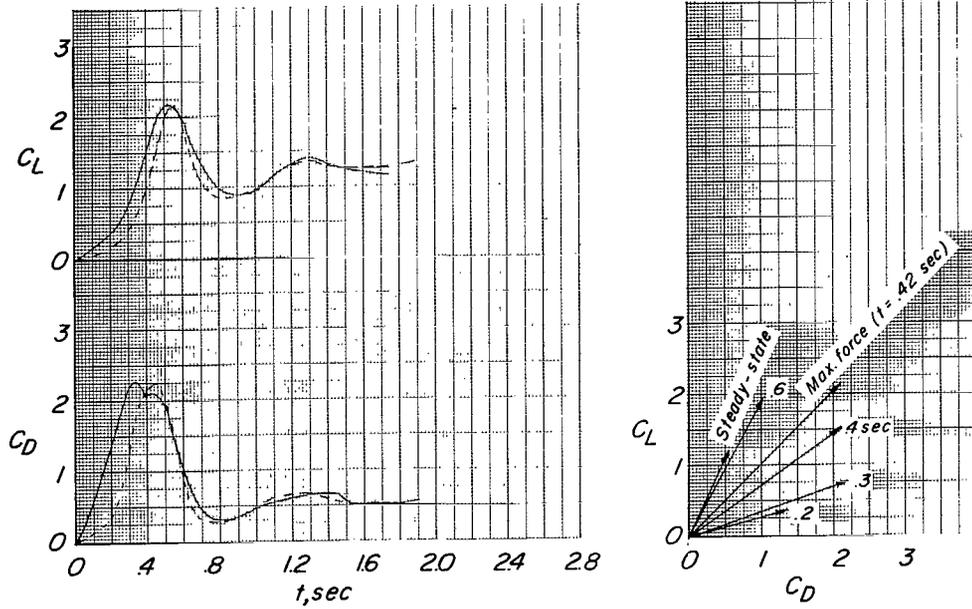
(a) Wing with overlapping slots.
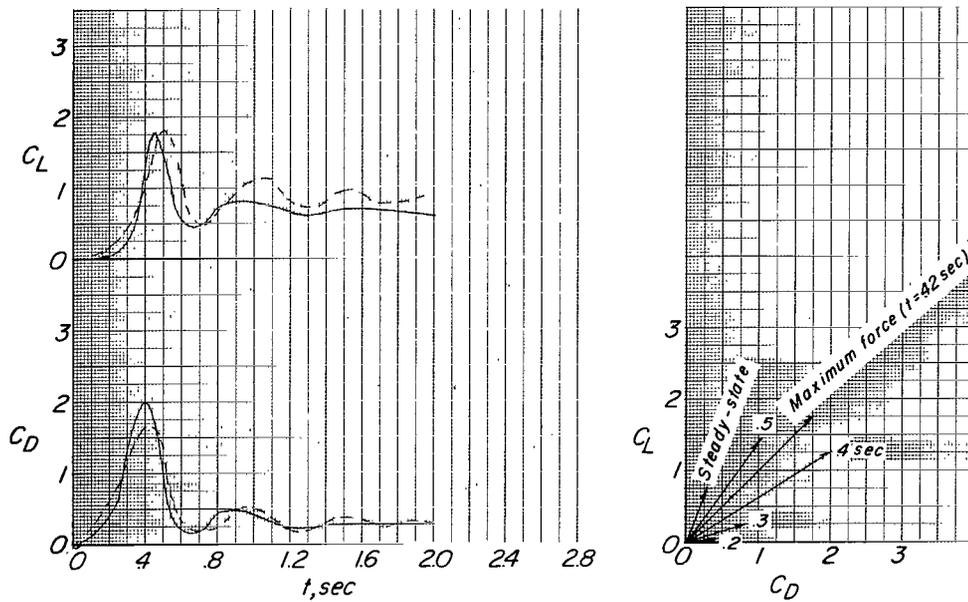
(b) Wing with slots toward the rear and center.

Figure 11.- Time histories of lift and drag coefficient for two slotted models.
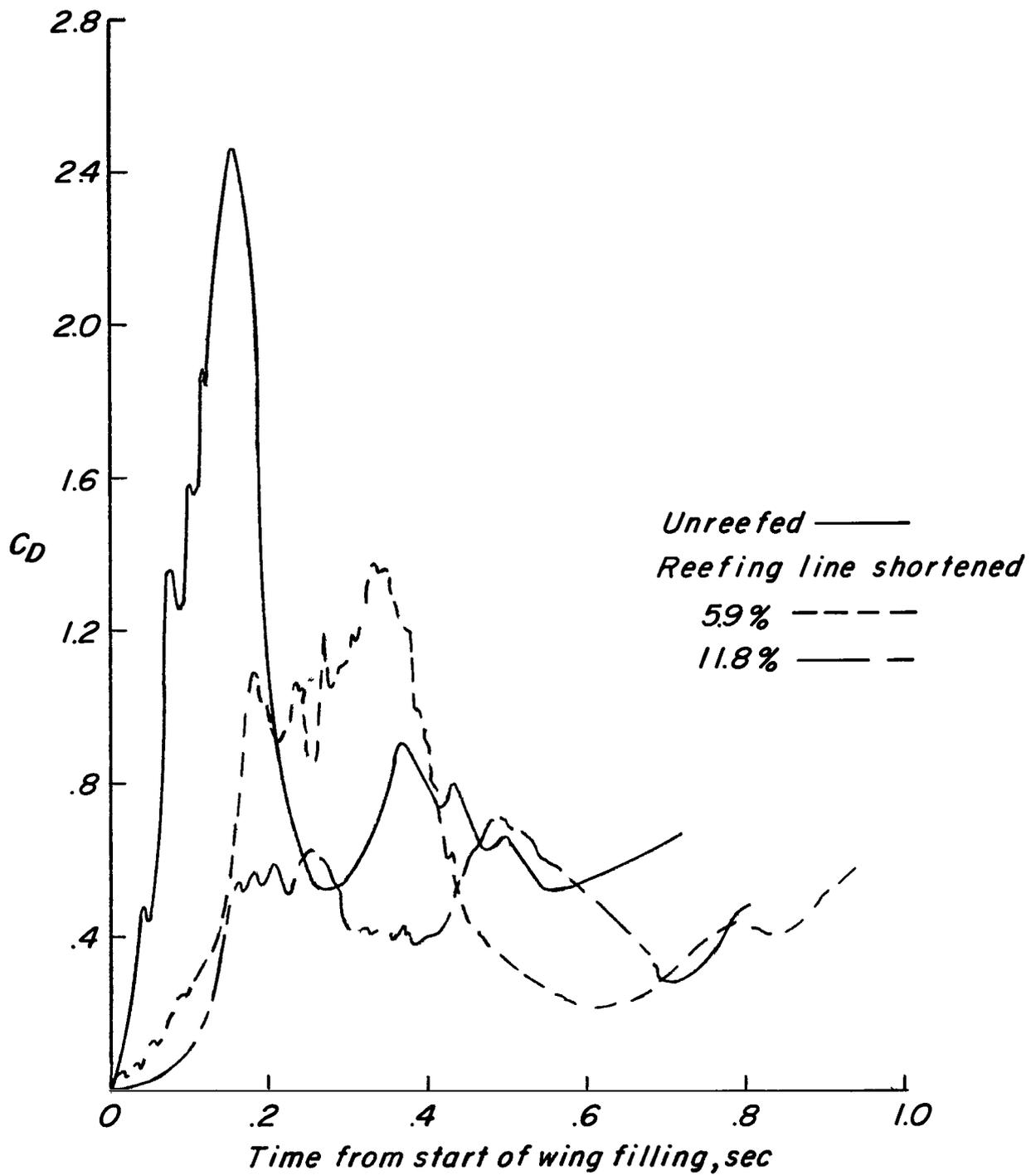
Figure 12.- Effect of reefing on drag-coefficient time history.
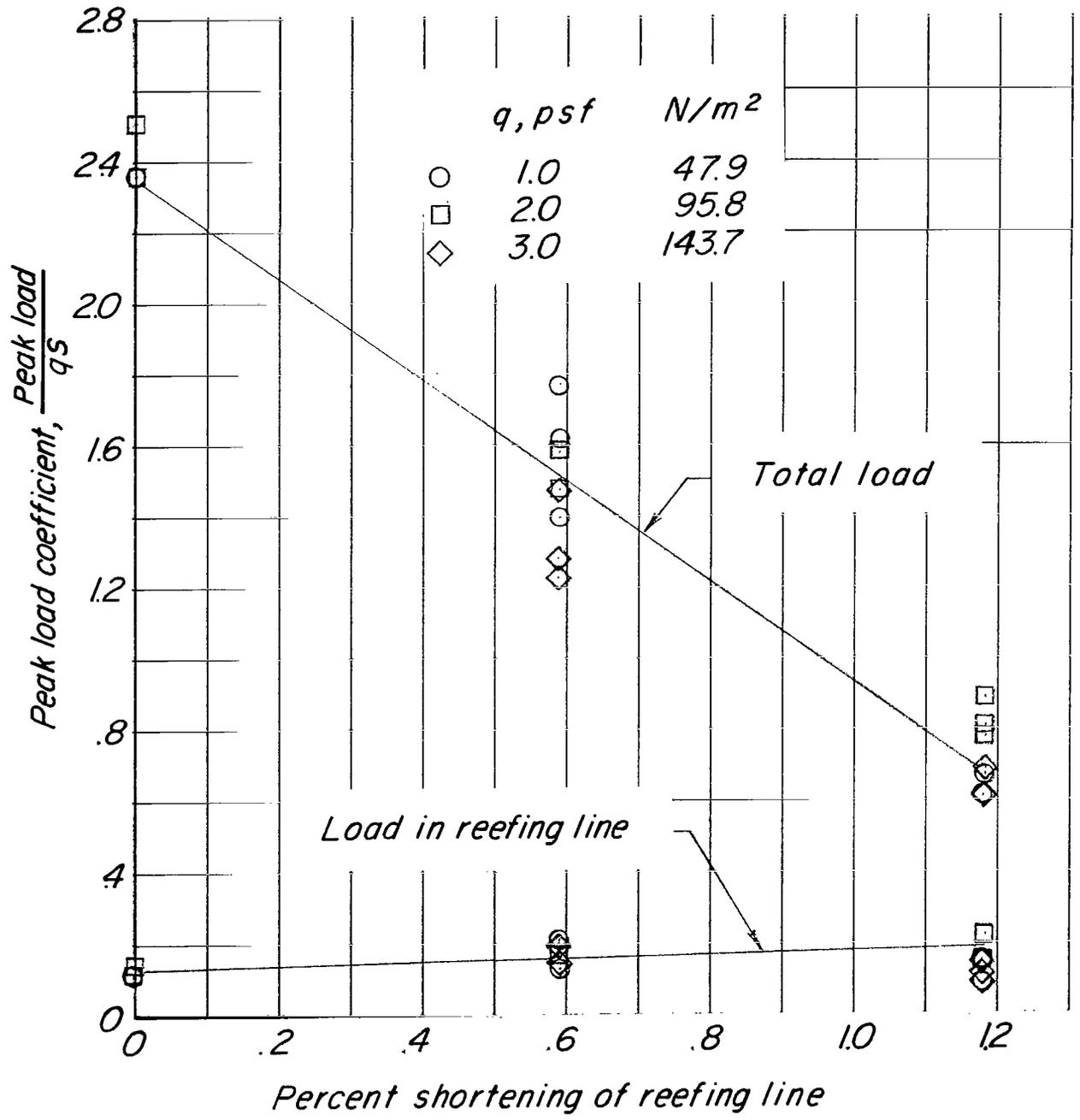
Figure 13.- Effect of reefing on maximum drag coefficient and maximum force in reefing line.

FIRST CLASS MAIL

CSU 001 27   01 3US   69033 00903
AIR FORCE WEAPONS LABORATORY/AFWL/
KIRTLAND AIR FORCE BASE, NEW MEXICO 87117

ATT E. LOU BOWMAN, ACTING CHIEF TECH. LIB

"The aeronautical and space activities of the United States shall be conducted so as to contribute . . . to the expansion of human knowledge of phenomena in the atmosphere and space. The Administration shall provide for the widest practicable and appropriate dissemination of information concerning its activities and the results thereof."

— NATIONAL AERONAUTICS AND SPACE ACT OF 1958

NASA SCIENTIFIC AND TECHNICAL PUBLICATIONS

TECHNICAL REPORTS: Scientific and technical information considered important, complete, and a lasting contribution to existing knowledge.

TECHNICAL NOTES: Information less broad in scope but nevertheless of importance as a contribution to existing knowledge.

TECHNICAL MEMORANDUMS: Information receiving limited distribution because of preliminary data, security classification, or other reasons.

CONTRACTOR REPORTS: Scientific and technical information generated under a NASA contract or grant and considered an important contribution to existing knowledge.

TECHNICAL TRANSLATIONS: Information published in a foreign language considered to merit NASA distribution in English.

SPECIAL PUBLICATIONS: Information derived from or of value to NASA activities. Publications include conference proceedings, monographs, data compilations, handbooks, sourcebooks, and special bibliographies.

TECHNOLOGY UTILIZATION PUBLICATIONS: Information on technology used by NASA that may be of particular interest in commercial and other non-aerospace applications. Publications include Tech Briefs, Technology Utilization Reports and Notes, and Technology Surveys.

Details on the availability of these publications may be obtained from:

SCIENTIFIC AND TECHNICAL INFORMATION DIVISION

NATIONAL AERONAUTICS AND SPACE ADMINISTRATION

Washington, D.C. 20546